Electronic Supplementary Information (ESI)

Game theory in molecular nanosensing system for rapid detection of Hg^{2+} in aqueous solutions

Nan Fang Nie, Xin Xing Zhang, Chu Shan Fang, Qiu Yan Zhu, Jiao Yang Lu, Fu Rui Zhang, Qing Feng Yao, Wei Tao Huang, Xue Zhi Ding, and Li Qiu Xia

1. Comparison of Fluorescence Quenching Ability of CoOOH to Different Fluorescence Dyes

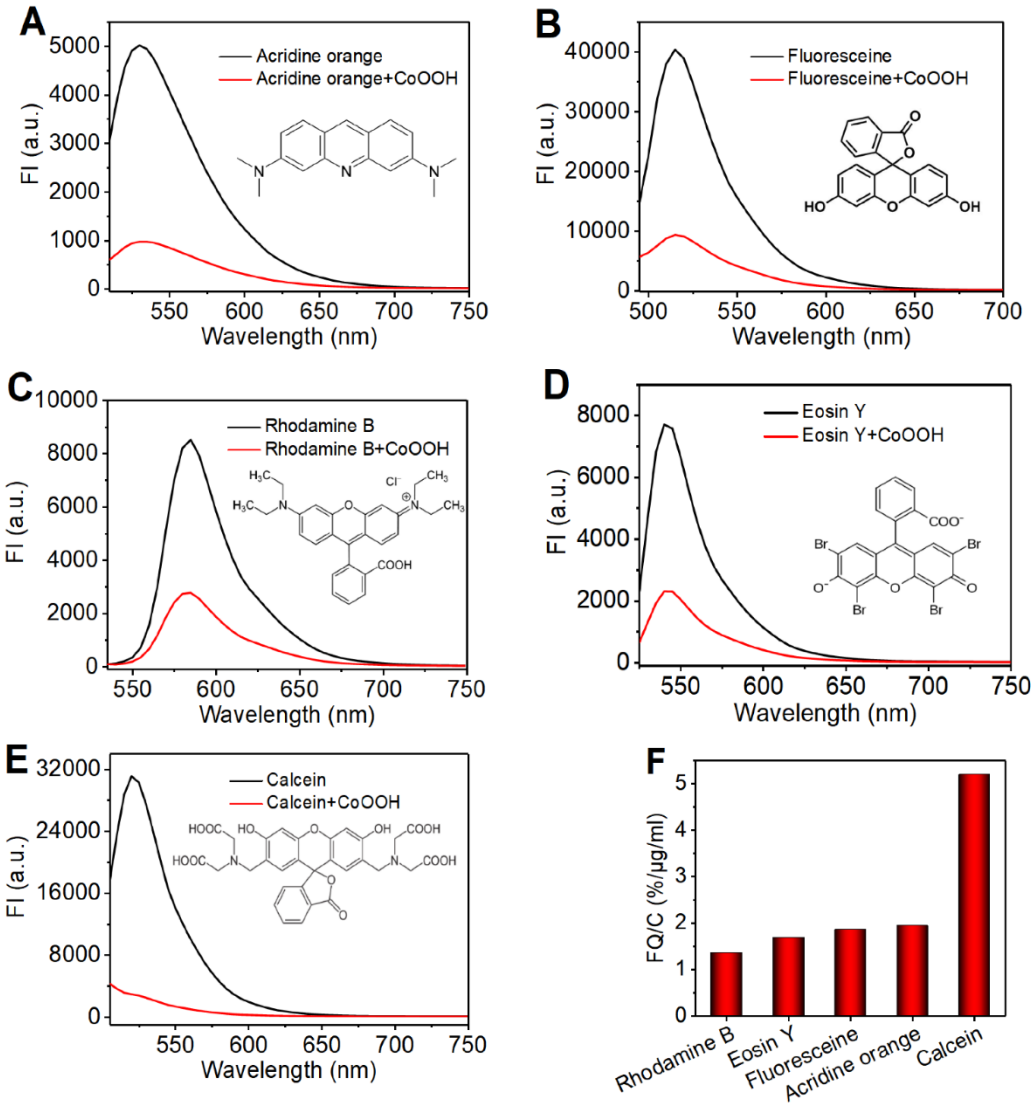

Figure S1. (**A-E**) Fluorescence emission spectra of five kinds of fluorescence dyes (acridine orange, fluoresceine, Rhodamine B, eosin Y, calcein) in Tris–HCl buffer (5 mM, pH 7.4) in the presence and absence of CoOOH nanosheets. The experimental conditions as follows: (**A**) acridine orange (2 mL, 0.1 mM) and CoOOH (400 μL, 0.25 mg/mL); (**B**) fluoresceine (2 mL, 0.01 mM) and CoOOH (400 μL, 0.25 mg/mL); (**C**) rhodamine B (2 mL, 0.1 mM) and CoOOH (500 μL, 0.25 mg/mL); (**D**) eosin Y (2 mL, 0.1 mM) and CoOOH (400 μL, 0.25 mg/mL); (**E**) (2 mL, 0.01 mM) and CoOOH (150 μL, 0.25 mg/mL). (F) Comparison of the fluorescence quenching ability of CoOOH to different fluorescence dyes.

2. Characterization of CoOOH Nanosheets

The CoOOH nanosheets prepared according to the literature method were characterized by TEM, SEM, and UV-Vis spectrometer. The TEM and SEM images in Figure S2A showed that the morphology of CoOOH nanosheets was mainly hexagonal, which agreed well with the literature report.[1] As shown in Figure S2B, the CoOOH nanosheets exhibited an extensive absorption band from 300 nm to 700 nm (black line) which overlapped with the fluorescence emission spectrum of T33 (red line), indicating that the CoOOH nanosheets can serve as a potential quencher to various fluorescence molecules, such as FAM, acridine orange, fluoresceine, rhodamine B, eosin Y, and calcein (Figure S1). These results proved that the successfully synthesized CoOOH nanosheets had unique quenching ability.

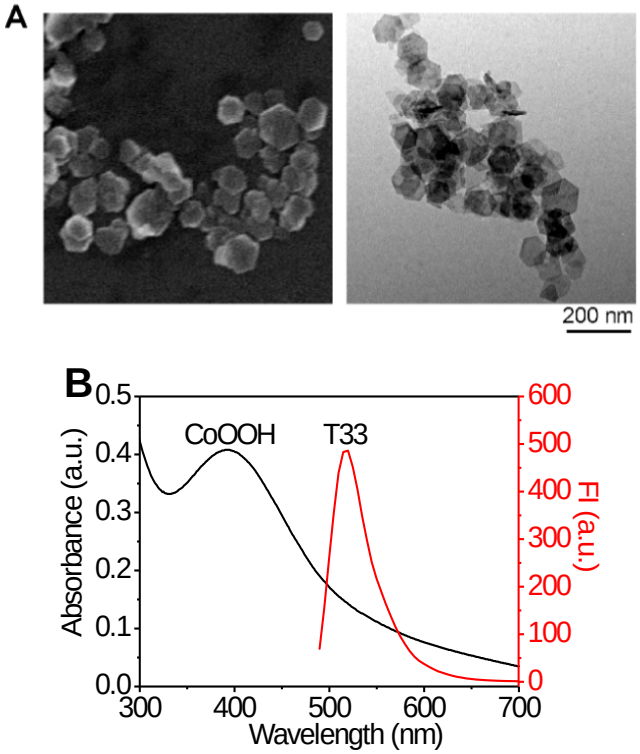

Figure S2. (A) TEM and SEM images of the prepared CoOOH nanosheets. (B) UV-Vis absorbance spectrum of CoOOH nanosheets (10 μg/ml) and fluorescence spectrum of T33 (100 nM).

3. Comparison of ζ-potential for CoOOH, T33–CoOOH, and T33–CoOOH–Hg^{2+} Mixtures

The result of Zeta potential (Figure S3) shows that positively charged CoOOH nanosheets and negatively charged T33 form a negatively charged T33–CoOOH complex through electrostatic adsorption. After addition of Hg^{2+}, the negative charge of the three complexes is reduced accordingly.

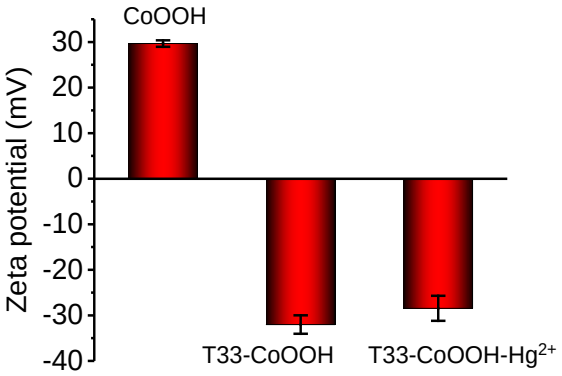

Figure S3. Comparison of ζ-potential for CoOOH, T33–CoOOH, and T33–CoOOH–Hg^{2+} mixtures.

4. Comparison of Fluorescence Changes of Free Fluorescein, T33, and T33–CoOOH Complexes on the Different Concentration of Hg^{2+}

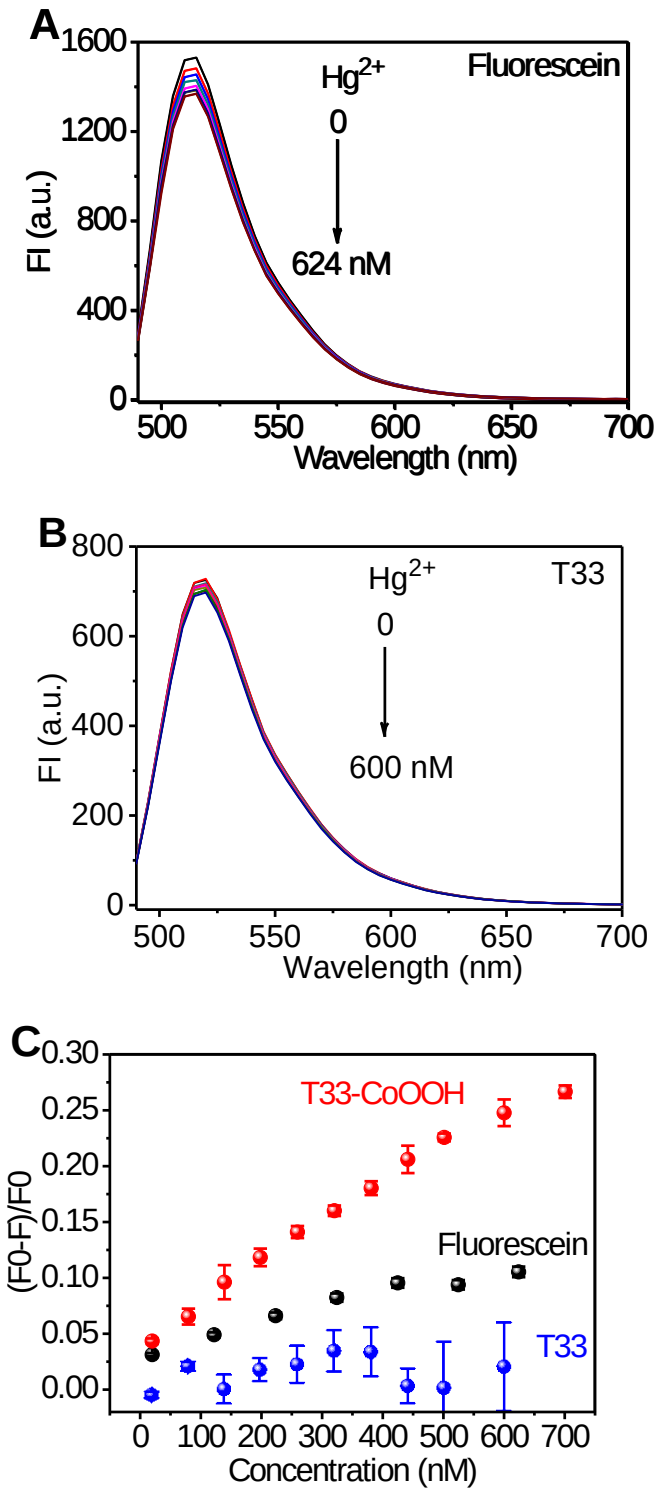

Figure S4. Fluorescence emission spectra of (**A**) free fluorescein sodium (100 nM) and (**B**) T33 (100 nM) upon addition of various concentrations of Hg^{2+}. (**C**) Comparison of the fluorescence changes (F0–F)/F0 at 520 nm of free fluorescein sodium (100 nM), T33 (100 nM) and T33–CoOOH complexes (100 nM:4.60 μg/ml) on the different concentration of Hg^{2+}.

5. Optimization of Experimental Conditions

In order to better sensing sensitivity, the concentration of CoOOH nanosheets and reaction time were optimized. Figure S5A indicated that the fluorescence responses of T33 in the presence of different concentration of CoOOH nanosheets. With the increased concentration of CoOOH nanosheets, fluorescence intensity of T33 gradually decreased. The fluorescence quenching ratio and the concentration of CoOOH nanosheets presented a linear relationship in the range of 0 to 9.38 μg/ml. The fluorescence changes of the T33–CoOOH complex to Hg^{2+} (2 μM) reached maximal values (Figure S5B) when the concentration of CoOOH was 4.69 μg/ml (T33, 100 nM). Therefore, 4.69 μg/ml was considered to be the optimized concentration for CoOOH nanosheets.

Fluorescence changes as a function of reaction time were monitored to study the kinetic behavior of the T33 with CoOOH nanosheets and T33–CoOOH complexes with Hg^{2+}. Figure S6A revealed that the fluorescence of T33 was quickly quenched and reached equilibrium after 4 min upon addition of CoOOH nanosheets. Whereas the reaction equilibrium time between T33–CoOOH complex and Hg^{2+} was 3 min (Figure S6B). Therefore, we respectively choose 4 min for preparing T33–CoOOH complex and 3 min for detection Hg^{2+}.

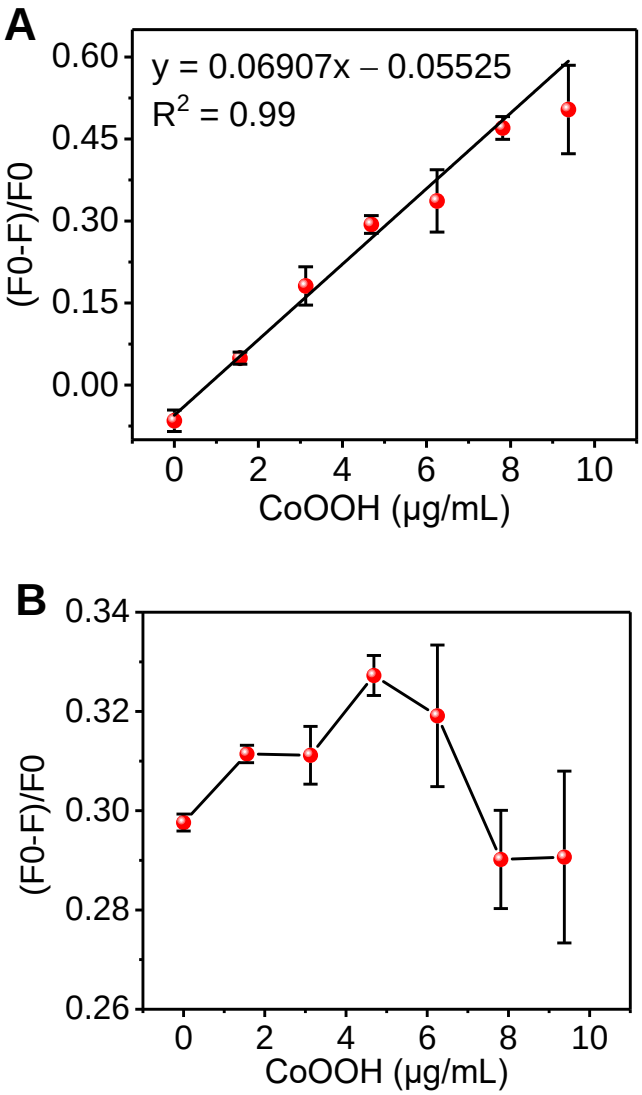

Figure S5. (**A**) The fluorescence quenching ratio of FAM-labeled T33 (100 nM) in the presence of different concentrations of CoOOH nanosheets (0, 1.56, 3.13, 4.69, 6.25, 7.81, 9.38 μg/ml). (**B**) The fluorescence changes of different ratio of T33–CoOOH complex to Hg^{2+} (2 μM).

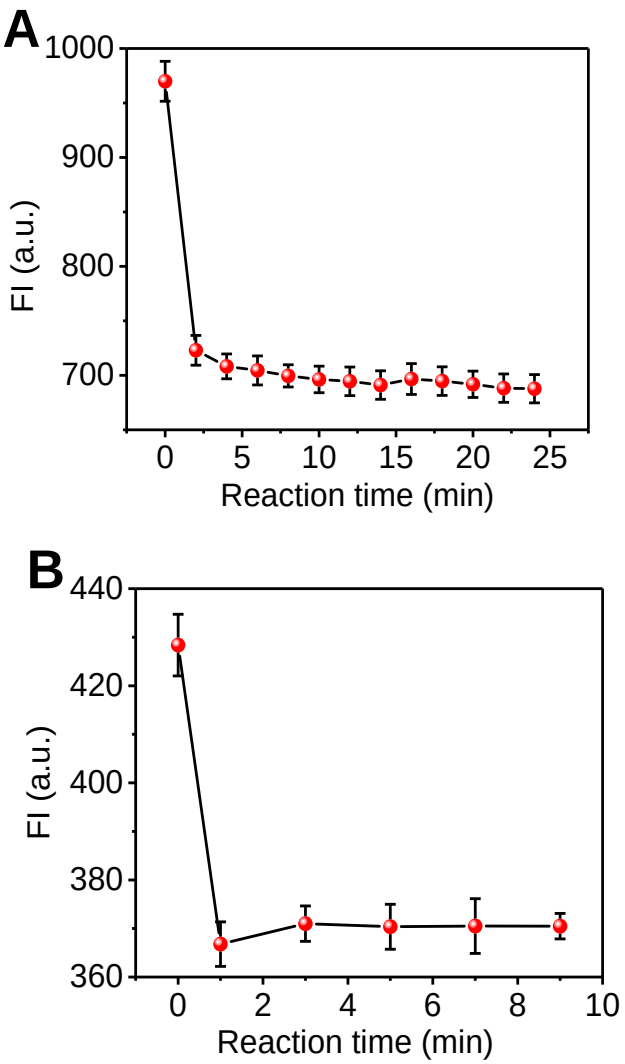

Figure S6. (**A**) Time dependence of fluorescence intensity at 520 nm for the FAM-labeled T33 in the presence of CoOOH. (**B**) Fluorescence response of T33–CoOOH complex in the presence of Hg^{2+} as a function of time. (T33: 100 nM, CoOOH: 4.69 μg/ml, Hg^{2+}: 98 nM).

6. Competition Experiment and the Interference of Anions

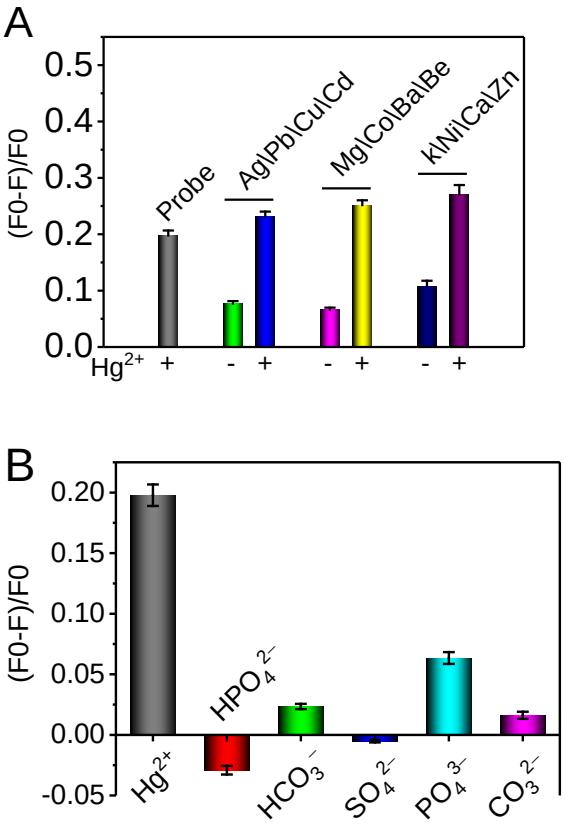

Figure S7. (**A**) Fluorescence response of this sensing system upon the addition of different metal ion mixtures and subsequent addition of Hg^{2+} (Hg^{2+}: 600 nM, other metal ions: 1.2 μM). (**B**) The fluorescence response of T33–CoOOH complex (100 nM:4.69 μg/ml) to common anions (HPO_4^{2-}, HCO_3^-, SO_4^{2-}, PO_4^{3-}, CO_3^{2-}: 1.2 μM, Hg^{2+}: 600 nM).

7. T33–CoOOH Complexes for Detection of A33 DNA.

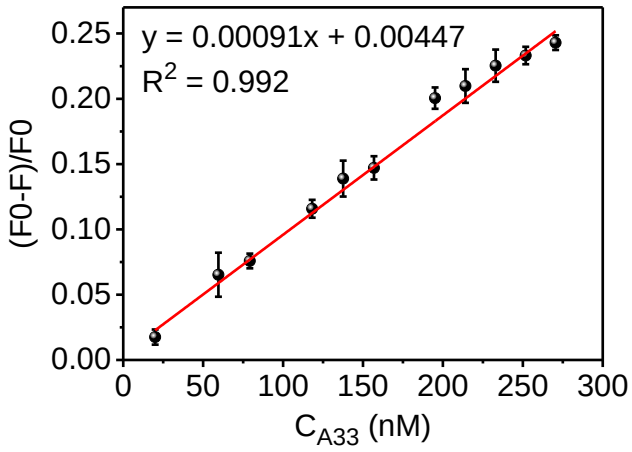

Figure S8. The linear relationship between fluorescence changes (F0–F)/F0 of T33–CoOOH complexes (100 nM:4.60 μg/ml) with the A33 concentrations in the range from 20 to 270 nM (20, 60, 80, 118, 138, 157, 195, 214, 233, 252, 270 nM). All measurements were done in 5 mM Tris–HCl buffer solution (pH 7.4).

8. Comparison of the Detection Limit and Linear Ranges of Other Reported Hg^{2+} Assays

Table S1. Comparison of the detection limit and linear ranges of other reported Hg^{2+} assays.

Probe	Detection limit	Linear range	Ref.
Thymine-rich ssDNA-functioned AuNPs	40 nM	96~6400 nM	2
AgNPs	2.2 μM	10~100 μM	3
Rhodamine-based fluorescent probe	15.7 nM	0.1~5 μM	4
Rhodamine-based fluorescent probe	50 nM	0~10 μM	5
Naphthalimide diimide-based fluorescent probe	1.3 μM	No given	6
Thymine-rich DNA	40 nM	40~100 nM	7
DNA-functionalized AuNPs	250 nM	0.5~5 μM	8
Conjugated polymer nanoparticles	about 3.5 nM	0~570 nM	9
T33/reporter conjugates	10 nM	25~500 nM	10
Thrombin-binding aptamer	5 nM	10~200 nM	11
T33–CoOOH complexes	7.94 nM	20~600 nM	This work

References

1. Li, N.; Li, Y.H.; Han, Y.Y.; Pan, W.; Zhang, T.T.; Tang, B. A Highly Selective and Instantaneous Nanoprobe for Detection and Imaging of Ascorbic Acid in Living Cells and in Vivo. *Anal. Chem.* **2014,** *86*, 3924–3930.
2. Wang, H.; Wang, Y.; Jin, J.; Yang, R., Gold Nanoparticle-Based Colorimetric and "Turn-On" Fluorescent Probe for Mercury(II) Ions in Aqueous Solution. *Anal. Chem.* **2008,** *80*, 9021–9028.
3. Farhadi, K.; Forough, M.; Molaei, R.; Hajizadeh, S.; Rafipour, A. Highly selective Hg2+ colorimetric sensor using green synthesized and unmodified silver nanoparticles. *Sensors Actuators B: Chem.* **2012,** *161*, 880–885.
4. Hu, J.; Hu, Z.; Cui, Y.; Zhang, X.; Gao, H.W.; Uvdal, K. A rhodamine-based fluorescent probe for Hg2+ and its application for biological visualization. *Sensors Actuators B: Chem.* **2014,** *203*, 452–458.
5. Shang, G.Q.; Gao, X.; Chen, M.X.; Zheng, H.; Xu, J.G. A Novel Hg2+ Selective Ratiometric Fluorescent Chemodosimeter Based on an Intramolecular FRET Mechanism. *Journal of Fluorescence* **2008,** *18*, 1187–1192.
6. Zong, L.; Xie, Y.; Li, Q.; Li, Z. A new red fluorescent probe for Hg 2+ based on naphthalene diimide and its application in living cells, reversibility on strip papers. *Sensors Actuators B: Chem.* **2017,** *238*, 735–743.
7. Liu, J.; Lu, Y. Rational Design of "Turn-On" Allosteric DNAzyme Catalytic Beacons for Aqueous Mercury Ions with Ultrahigh Sensitivity and Selectivity. *Angew. Chem. Int. Ed.* **2007,** *46*, 7587–7590.
8. Liu, C.W.; Hsieh, Y.T.; Huang, C.C.; Lin, Z.H.; Chang, H.T. Detection of mercury(ii) based on Hg2+–DNA complexes inducing the aggregation of gold nanoparticles. *Chem. Commun.* **2008,** 19, 2242.
9. Childress, E.S.; Roberts, C.A.; Sherwood, D.Y.; LeGuyader, C.L.M.; Harbron, E.J. Ratiometric Fluorescence Detection of Mercury Ions in Water by Conjugated Polymer Nanoparticles. *Anal. Chem.* **2012,** *84*, 1235–1239.
10. Lin, Y.W.; Liu, C.W.; Chang, H.T., Fluorescence detection of mercury(II) and lead(II) ions using aptamer/reporter conjugates. *Talanta* **2011,** *84*, 324–329.
11. Liu, C.W.; Huang, C.C.; Chang, H.T. Highly Selective DNA-Based Sensor for Lead(II) and Mercury(II) Ions.

Anal. Chem. **2009,** *81,* 2383–2387.